Calcium and strontium thiobarbiturates with discrete and polymeric structures

N.N. Golovnev, M.S. Molokeev, S.N. Vereshchagin & V.V. Atuchin

Taylor & Francis
Taylor & Francis Group

Calcium and strontium thiobarbiturates with discrete and polymeric structures

N.N. GOLOVNEV†, M.S. MOLOKEEV*‡, S.N. VERESHCHAGIN§ and
V.V. ATUCHIN¶

†Department of Chemistry, Siberian Federal University, Krasnoyarsk, Russia
‡Laboratory of Crystal Physics, Kirensky Institute of Physics, Krasnoyarsk, Russia
§Laboratory of Catalytic Conversion of Small Molecules, Institute of Chemistry and Chemical
Technology, Krasnoyarsk, Russia
¶Laboratory of Optical Materials and Structures, Institute of Semiconductor Physics, Novosibirsk,
Russia

Three new alkaline earth metal complexes, $[Ca_2(H_2O)_8(\mu_2\text{-HTBA-O,O'})_2(HTBA\text{-}O)_2]$ (**1**), $[Ca(H_2O)_5(HTBA\text{-}O)_2]\cdot 2H_2O$ (**2**), and $[Sr(H_2O)_4(\mu_2\text{-HTBA-O,S})_2]_n$ (**3**) (H_2TBA = 2-thiobarbituric acid, $C_4H_4N_2O_2S$), were synthesized and characterized by FT-IR spectroscopy, TG-DSC, and single-crystal and powder X-ray diffraction analysis. The single-crystal X-ray diffraction data revealed that **1** and **2** are discrete structures, whereas **3** is a polymer. In **1** and **2**, Ca^{2+} is seven-coordinate and forms a monocapped trigonal prism. In **1**, the prisms are pairwise connected with the assistance of two $[\mu_2\text{-HTBA-O,O'}]^-$ ligands. In **3**, Sr^{2+} is coordinated by four monodentate $HTBA^-$ via S or O donors and four waters, with the formation of a distorted square antiprism. The antiprisms are connected by $\mu_2\text{-O,S}$ bridging $HTBA^-$. Hydrogen bonding involving coordinated water and π–π interactions plays an important role in construction of the supramolecular 3-D structures in **1**–**3**. Infrared spectroscopic data supported the structural data. The thermal stability of **1**–**3** decreases in the order **1** > **2** > **3**. Dehydration of **1**–**3** was a multi-step process, followed by exothermic oxidative degradation of the 2-thiobarbiturate moiety between 290 and 800 °C.

Keywords: Calcium; Strontium; 2-Thiobarbituric acid; Crystal structure; Thermal decomposition; IR spectroscopy

1. Introduction

The growing interest in the coordination chemistry of s-block elements has been demonstrated by several recent reviews [1–3]. The coordination polymers have attracted much attention because of their intriguing topology and promising applications in catalysis, adsorption (gas storage), and separation technologies [4–6]. Compared to the extensive chemistry of coordination polymers based on transition metals, the coordination chemistry of group 2 metals with organic linkers is relatively less explored. Because of the large ionic radius of alkaline earth metals such as calcium and strontium, these cations have larger coordination numbers compared to those of transition metal ions.

---

*Corresponding author. Email: msmolokeev@mail.ru
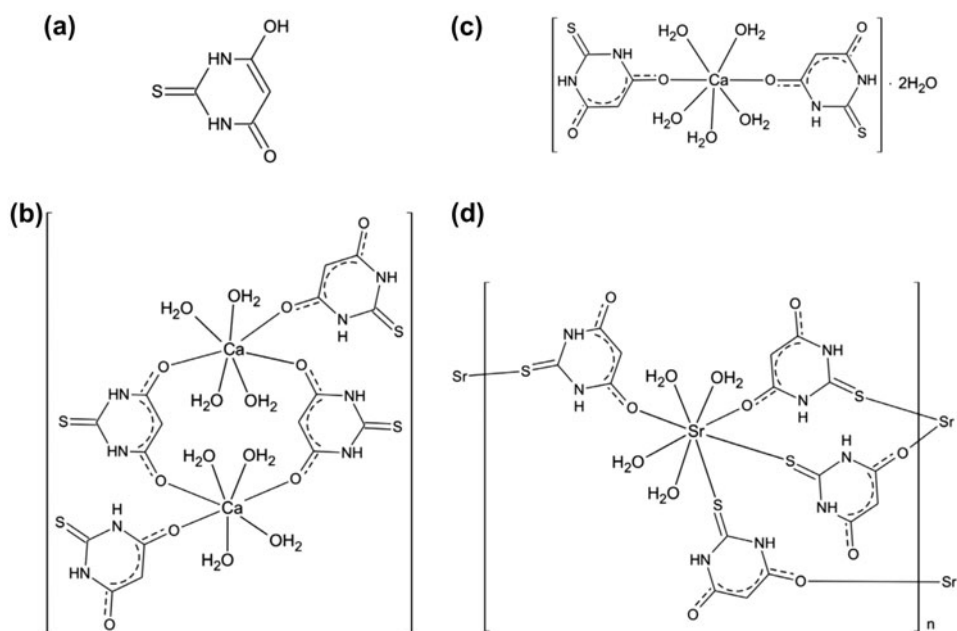
Scheme 1. Structure of (a) the enol form of 2-thiobarbituric acid; (b) $Ca_2(H_2O)_8(\mu_2\text{-HTBA-O,O'})_2(\text{HTBA-O})_2$, **1**; (c) $[Ca(H_2O)_5(\text{HTBA-O})_2]\cdot 2H_2O$, **2**; (d) $[Sr(H_2O)_4(\mu_2\text{-HTBA-O,S})_2]_n$, **3**.

2-thiobarbituric acid (2-thioxodihydropyrimidine-4,6(1H,5H)-dione, H_2TBA) (scheme 1(a)) has important applications in pharmaceuticals and analytical chemistry [7–9]. It has many possible tautomeric structures [10, 11] and very desirable properties for forming supramolecular structures [3]. For oxophilic s-block metals, the $HTBA^-$ ligand containing O and O′ donors could be a useful linker for the preparation of coordination polymers, since the metals can be linked into an extended chain with bridging $HTBA^-$. However, structural information on the compounds of H_2TBA with alkaline earth metals is very scarce [12]. All these factors make the synthesis of coordination polymer networks with alkaline earth metal cations a strategic challenge [2]. Also, characterization of alkaline earth compounds with thiobarbiturates is the area of continuous interest because of the relevance of new compounds with potentially valuable pharmaceutical properties [13]. The fundamental interest of our present study is the exploration of the changes in the solid-state structure of thiobarbiturate complexes induced by the alkaline earth cation substitution.

2. Experimental

2.1. *Materials and synthesis*

2-thiobarbituric acid [CAS 504-17-6] was commercially available from Fluka. The sample was carefully dried under vacuum and then used without special purification. $CaCO_3$ and $SrCO_3$ were obtained as reagent grade materials and used without purification. All complexes were readily prepared by neutralization of thiobarbituric acid with the corresponding alkaline-earth metal carbonate in an aqueous solution. The ligand (0.002 M) was mixed with

the metal carbonate (0.001 M) in water (5 cm^3). The mixtures were stirred for 5 h at 60 °C. Pale pink precipitates formed in the solutions were filtered, washed several times with EtOH, and dried in air at room temperature. The powder products were soluble in water. Crystals suitable for X-ray analysis were grown by continuous evaporation of the filtrates at 60 °C (for **1** and **3**) or at 20 °C (for **2**). The chemical analyzes were carried out with a HCNS-0 EA 1112 Flash Elemental Analyser.

Anal. Calcd for C$_{16}$H$_{28}$Ca$_2$N$_8$O$_{16}$S$_4$ (**1**): C, 24.12; H, 3.54; N, 14.06; S, 16.10. Found: C, 23.98; H, 3.71; N, 13.88; S, 16.02 (%). Yield = 0.32 g (80%).

Anal. Calcd for C$_8$H$_{20}$CaN$_4$O$_{11}$S$_2$ (**2**): C, 21.24; H, 4.46; N, 12.38; S, 14.17. Found: C, 21.02; H, 4.71; N, 12.41; S, 14.00 (%). Yield = 0.37 g (82%).

Anal. Calcd for C$_8$H$_{14}$N$_4$O$_8$S$_2$Sr (**3**): C, 21.55; H, 3.16; N, 12.56; S, 14.38. Found: C, 21.18; H, 3.40; N, 12.24; S, 14.11 (%). Yield = 0.38 g (85%).

2.2. *Physical measurements*

IR spectra (figure S1) were recorded for the powder samples as KBr pellets on a Bruker Vector-22 Fourier spectrometer from 400 to 4000 cm^{-1}. The spectral resolution during measurements was 5 cm^{-1}. Thermal behavior was studied by simultaneous thermal analysis using a Netzsch STA Jupiter 449C with on-line Aeolos QMS 403C mass spectrometer under dynamic argon-oxygen atmosphere (20 vol.% O$_2$) at a temperature ramp rate of 10° min^{-1}. Powder X-ray diffraction data were obtained using the diffractometer D8 ADVANCE (Bruker) equipped with a VANTEC detector with a Ni filter. The measurements were produced using Cu Kα radiation.

2.3. *Single crystal X-ray diffraction analysis*

The determination of the unit cell and the data collection for **1–3** were performed on a Bruker SMART APEX II diffractometer with graphite-monochromated Mo-Kα radiation

Table 1. Crystal, data collection, and refinement parameters for **1–3**.

	1	2	3
Empirical formula	C$_{16}$H$_{28}$Ca$_2$N$_8$O$_{16}$S$_4$	C$_8$H$_{20}$CaN$_4$O$_{11}$S$_2$	C$_8$H$_{14}$N$_4$O$_8$S$_2$Sr
Molecular mass	796.86	452.50	445.99
Crystal system	Triclinic	Orthorhombic	Monoclinic
Space group	$P\bar{1}$	*Pbcn*	$P2_1/n$
a (Å)	8.4180(8)	12.981(2)	12.9753(8)
b (Å)	9.1422(9)	8.400(1)	7.2255(5)
c (Å)	10.6741(11)	17.069(2)	16.434(1)
α (°)	76.070(1)	90	90
β (°)	84.551(1)	90	94.883(1)
γ (°)	70.733(1)	90	90
Volume (Å^3)	752.6(1)	1861.2(4)	1535.1(2)
Z	2	4	4
Calculated density (g cm^{-3})	1.758	1.615	1.930
F (000)	412	944	640
Reflections collected	7398	16,498	14,393
Independent reflections	3898	2551	4103
Data/restraints/parameters	3898/0/233	2551/12/141	4103/2/234
Goodness of fit on F^2	1.036	1.063	1.010
Final R indices [$I>2\sigma(I)$]	$R_1 = 0.0405$	$R_1 = 0.0312$	$R_1 = 0.0338$
	$wR_2 = 0.0822$	$wR_2 = 0.0807$	$wR_2 = 0.0660$
R indices (all data)	$R_1 = 0.0680$	$R_1 = 0.0396$	$R_1 = 0.0567$
	$wR_2 = 0.0960$	$wR_2 = 0.0863$	$wR_2 = 0.0729$

Table 2. Selected bond distances (Å) and angles (°) for **1–3**.

Ca(HTBA)$_2$(H$_2$O)$_4$ (**1**)		[Ca(HTBA)$_2$(H$_2$O)$_5$]·2H$_2$O (**2**)		Sr(HTBA)$_2$(H$_2$O)$_4$ (**3**)	
Ca–O1a	2.355(2)	Ca–O1	2.324(1)	Sr–O2	2.523(2)
Ca–O2w	2.390(3)	Ca–O5	2.375(2)	Sr–O2b	2.536(2)
Ca–O1w	2.395(2)	Ca–O3	2.392(1)	Sr–O1	2.553(2)
Ca–O3w	2.411(3)	Ca–O4	2.498(1)	Sr–O4	2.567(2)
Ca–O4w	2.422(2)			Sr–O1a	2.572(2)
Ca–O1b	2.446(2)			Sr–O3	2.583(2)
Ca–O2a	2.474(2)			Sr–S1^i	3.1668(7)
				Sr–S2^{ii}	3.3533(7)
C4a–O1a	1.254(3)	C4–O1	1.261(2)	C4a–O1a	1.266(3)
C4b–O1b	1.275(3)			C4b–O1b	1.261(3)
C6a–O2a	1.269(3)	C6–O2	1.271(3)	C6a–O2a	1.274(3)
C6b–O2b	1.263(3)			C6b–O2b	1.271(3)
C4a–C5a	1.396(3)	C4–C5	1.394(2)	C4a–C5a	1.395(3)
C4b–C5b	1.387(3)			C4b–C5b	1.394(3)
C5a–C6a	1.381(3)	C5–C6	1.390(2)	C5a–C6a	1.383(3)
C5b–C6b	1.395(3)			C5b–C6b	1.387(3)
C4a–C5a–C6a	121.6(2)	C4–C5–C6	120.1(1)	C4a–C5a–C6a	121.0(2)
C4b–C5b–C6b	120.6(2)			C4b–C5b–C6b	121.4(2)

Note: Transformations of the asymmetric unit for **3**: (i) $x - \frac{1}{2}$; $3/2 - y$, $z - \frac{1}{2}$; (ii) $1 - x$, $2 - y$, $- z$.

($\lambda = 0.71073$ Å) at 296(2) K using the ω–2θ scan technique. The structures were solved by direct methods with SHELXS-97 [14] and refined against F^2 by full-matrix least-squares using SHELXL-97. All non-hydrogen atoms were refined anisotropically. All hydrogens of HTBA$^-$ were positioned by difference Fourier maps and refined using a riding model with restraints and the thermal parameters set equal to 1.2 × Ueq of the parent atoms. All water hydrogen atoms were positioned by difference Fourier maps. For **1**, all these atoms were refined without restraints. For **2**, they were refined with the distance restraint of d(O–H) = 0.9 Å. For **3**, the hydrogen atoms bonded to O4 were refined with the distance restraint of d(O–H) = 0.9 Å, and the other water hydrogen atoms were refined without restraints. A summary of crystal, data collection, and refinement parameters is given in table 1. Selected bond distances and angles for **1–3** are listed in table 2. The parameters for the intermolecular hydrogen bonds in **1–3** are summarized in table 3.

3. Results and discussion

3.1. *Crystal structure of bis[(μ$_2$-2-thiobarbiturato-O,S)-(2-thiobarbiturato-O)]octaaqua-dicalcium(II), 1*

The single crystal X-ray diffraction experiment revealed a discrete structure for **1**. The asymmetric unit consists of one Ca^{2+} cationic center, two HTBA$^-$ ligands, and four water molecules, as shown in scheme 1(b) and figure 1. The HTBA$^-$ anions (denoted as A and B) are nonequivalent, with anion A a μ$_2$-O,O′ bridging ligand and anion B a terminal, monodentate ligand. The Ca^{2+} cation is coordinated by seven O atoms from four water molecules and three HTBA$^-$ anions, forming a monocapped trigonal prism. The prisms are pairwise connected via the bridging HTBA$^-$ ligand, A. These discrete pairs form continuous chains

Table 3. Hydrogen bonding distances and angles for **1–3**.

Complex	Atoms	Distance (Å)	Angles (°)
1	O1w, H1aw⋯O1b[i]	2.662(3), 1.77(3)	170
	N3b, H3b⋯O2a	2.793(3), 1.96	163
	N3a, H3a⋯O2b[i]	2.982(3), 2.13	170
	O4w, H4bw⋯O2b[ii]	2.888(3), 2.10(3)	161
	O4w, H4aw⋯O1w[i]	2.830(3), 2.12(3)	151
	O3w, H3bw⋯O3b[iii]	2.884(3), 2.143(3)	166
	O2w, H2bw⋯S1[iv]	3.229(3), 2.48(4)	148
	N1a, H1a⋯S2	3.373(2), 2.54	163
	O1w, H1bw⋯S2[v]	3.271(2), 2.56(3)	156
	O2w, H2aw⋯S1[v]	3.333(3), 2.58(3)	164
2	N1, H1⋯O4[i]	2.917(2), 2.06	176
	N3, H3⋯O6[ii]	2.847(2), 1.99	172
	O4, H41⋯O6	2.826(2), 2.04(2)	160(2)
	O4, H42⋯O2[iii]	2.732(2), 1.89(2)	171(2)
	O5, H51⋯O2[iv]	2.809(2), 1.96(2)	167(1)
	O6, H61⋯O1[v]	3.008(2), 2.18(2)	162(2)
	O6, H62⋯O2[vi]	2.496(2), 1.91(2)	169(2)
	O3, H31⋯S[vii]	3.300(1), 2.54(2)	151(2)
	O3, H32⋯S[i]	3.252(1), 2.37(2)	175(2)
3	N1a, H1a⋯O2b[i]	2.799(3), 1.94	174
	N1b, H1b⋯O2a[ii]	2.858(3), 2.01	171
	O1, H11⋯O1b[iii]	2.751(3), 1.99(3)	166(4)
	O2, H21⋯O2a[iv]	2.799(3), 2.00(4)	174(3)
	O2, H22⋯O1b[iv]	2.988(3), 2.22(4)	168(3)
	O3, H31⋯O2a[v]	2.876(3), 2.07(4)	175(3)
	O3, H32⋯O1b[v]	2.972(3), 2.14(4)	168(3)
	O4, H41⋯O1a[vi]	2.820(3), 2.13(3)	139(3)
	N3b, H3b⋯S1[vii]	3.456(2), 2.60	179
	N3a, H3a⋯S2[viii]	3.393(2), 2.53	176
	O4, H42⋯S2[ix]	3.336(2), 2.51(3)	169(3)

Note: Transformations of the asymmetric unit: for **1** (i) $-x + 1$, $-y + 2$, $-z$; (ii) $x + 1$, $y-1$, z; (iii) $-x$, $-y + 2$, $-z$; (iv) $-x$, $-y + 2$, $-z + 1$; (v) $x + 1$, y, z. For **2** (i) $-x + 1$, y, $-z + 1/2$; (ii) $-x + 1$, $-y$, $-z$; (iii) x, $-y$, $z + 1/2$; (iv) $-x + 1$, $-y + 1$, $-z$; (v) $x - 1/2$, $y - 1/2$, $-z + 1/2$; (vi) $-x + 1/2$, $-y + 1/2$, $z - 1/2$; (vii) $-x + 1/2$, $-y + 1/2$, $-z$. For **3** (i) $x-1/2$, $-y + 3/2$, $z-1/2$; (ii) $x + 1/2$, $-y + 3/2$, $z + 1/2$; (iii) $x + 1/2$, $-y + 3/2$, $z - 1/2$; (iv) $-x + 3/2$, $y + 1/2$, $-z + 1/2$; (v) $-x + 3/2$, $y - 1/2$, $-z + 1/2$; (vi) $-x + 2$, $-y + 1$, $-z$; (vii) $x - 1$, y, z; (viii) $x + 1$, y, z; (ix) $1 - x$, $1 - y$, $-z$.

via hydrogen bonding along the $\overline{b} - \overline{c}$. direction (figure S4). Two μ₂-HTBA⁻ ligands, together with two Ca²⁺ cations, form a 12-membered ring (figure 1), and the Ca–Ca distance is 6.7548(9) Å. Similar rings were also observed in other related compounds, as found with the Mercury CSD 3.1 program (table S1). In these compounds, the metal–metal distances are in the range 5.51–8.95 Å, excluding one very short distance of 3.33 Å. This indicates the great flexibility of the ring due to its large size. The majority of the compounds listed in table S1 have a metal–metal distance of ~7 Å, consistent with that observed in **1**.

The Ca–O bond distances (table 2) range from 2.355(2) to 2.474(2) Å and are comparable to those reported for Ca–O (carbonyl) and Ca–O (aqua) bond distances in other seven-coordinate calcium complexes [12]. The Ca–O (carbonyl) bond distances are in the range 2.355–2.474 Å and the Ca–O (water) bond distances have a narrower range, 2.390–2.446 Å. For the carbonyl O atoms, the difference between the Ca–O1A bond distance [2.355(2) Å] and the bond distances for Ca–O1B [2.446(2) Å] and Ca–O2A [2.474(2) Å] can be explained by the involvement of the latter O atoms in hydrogen-bonding interactions, while there is no hydrogen bonding involving atom O1A.
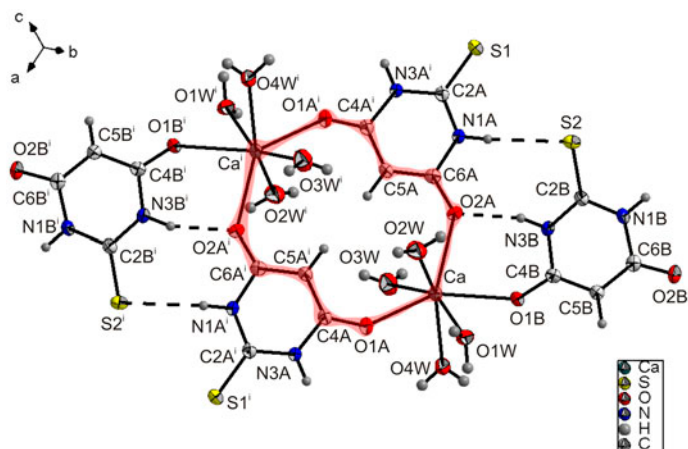
Figure 1. Crystal structure of **1** together with the labeling scheme. Symmetry code: (i) $1 - x$, $1 - y$, $1 - z$. The ellipsoids are drawn at the 50% probability level. The red line shows the 12-membered ring (see http://dx.doi.org/10.1080/19443994.2013.860450 for color version).
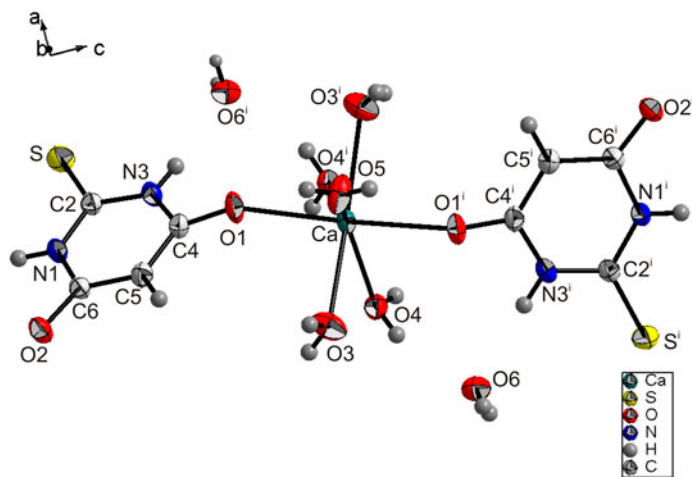

Figure 2. Crystal structure of **2** together with the labeling scheme. Symmetry code: (i) $1 - x$, y, $\frac{1}{2} - z$. The ellipsoids are drawn at the 50% probability level.

In the terminal HTBA$^-$ anion, the C6B–O2B distance in the noncoordinated carbonyl group is 1.263(2) Å and the corresponding distance in the coordinated carbonyl group, C4B–O1B, is 1.275(3) Å. This indicates charge delocalization in the HTBA$^-$ ligand. In the bridging HTBA$^-$ ligand, the C6A–O2A distance [1.269(3) Å] is a little longer than the C4A–O1A distance [1.254(3) Å]. In both HTBA$^-$ anions, the C4–C5–C6 angle corresponds to sp^2 hybridization [121.6(2)° for A and 120.6(2)° for B]. Also, the C4A–C5A and C5A–C6A distances [1.396(3) Å, 1.381(3) Å] and C4B–C5B and C5B–C6B distances [1.387(3) Å, 1.395(3) Å] are close to the values typical for aromatic rings. The geometric parameters of the HTBA$^-$ anions compare well to those of other known metal thiobarbiturates [12, 15, 16].

Hydrogen bonding (figure S5a) and π–π interactions (figure S5b) play important roles in the structure of **1**. Ten hydrogen bonds (table 3) generate 3-D net. Hydrogen bonds N1A–H1A···S2, N3A–H3A···O2B, and N3B–H3B···O2A form 8-membered and 6-membered rings with the graph set notations $R_2^2(8)$ and $R_1^1(6)$, respectively (figure S5a). There are also 12-membered [$R_2^2(12)$] and 20-membered [$R_3^3(20)$] rings in **1** (figure S5a). The self-associated hydrogen bonds between two HTBA$^-$ ligands, which form the HTBA$^-$ anion network, were previously described for potassium complexes [15, 16]. In **1**, a "head-tail" π–π stacking interaction exists between the rings of bridging HTBA$^-$ ligands (figure S5b). The distance of 3.639(1) Å between the rings of neighboring HTBA$^-$ anions is comparable to those in potassium thiobarbiturate [16]. The powder pattern of **1** simulated from the single crystal data agrees well with the measured one (figure S2), indicating that the crystal structure is representative of the bulk structure.

3.2. *Crystal structure of bis(2-thiobarbiturato-O)pentaaqua-calcium(II) dehydrate, 2*

Bis(2-thiobarbiturato-O)-pentaaqua-calcium dihydrate (**2**) is also a discrete structure. The compound crystallizes in the orthorhombic space group *Pbcn* with four formula units in the unit cell. The asymmetric unit consists of one Ca^{2+} cation in the 4*c* position, one HTBA$^-$ anion with all atoms in the 8*d* position, three coordinated waters (two of them in 8*d* position and one in 4*c* position), and one lattice water in the 8*d* position (scheme 1(c) and figure 2). As in **1**, the Ca atom is seven-coordinate, surrounded by five water molecules and two O-bound HTBA$^-$ anions, with a monocapped trigonal prism coordination geometry. In **2**, contrary to **1**, all coordinated HTBA$^-$ ligands are terminal. The Ca–O distances span a range from 2.324(1) Å for Ca–O1 to 2.498(1) Å for Ca–O4 and are comparable to those found in **1** and other calcium complexes [12]. The Ca–O4 bond is the longest because the O4 atom is involved in three hydrogen bonds as a donor and acceptor, while the other O atoms are involved in hydrogen bonding either as a donor or as an acceptor. The C4–O1 [1.261(2) Å] and C6–O2 [1.271(3) Å] distances are almost equal, indicative of charge delocalization in the HTBA$^-$ ligand. The C4–C5–C6 angle [120.1(1)°] corresponds to sp^2 hybridization. The bond distances and angles in the HTBA$^-$ anion are comparable to those in other metal thiobarbiturates [12, 15, 16]. Nine hydrogen bonds (figure S6 and table 3) generate a 3-D net in **2**. All water molecules are involved in hydrogen bonding to carbonyl O atoms or thione S atoms of the HTBA$^-$ ligands. There are no self-associated hydrogen bonds between HTBA$^-$ ligands as is found in **1**. Discrete complexes of **2** form layers in the plane determined by vectors $\vec{c}$ and $\vec{a} + \vec{b}$ (figure S6). The layers are joined together by the 3-D hydrogen-bonding network. The hydrogen bonds N–H···O, OW–H···OW, and OW–H···S generate 8-membered [$R_2^1(8)$], 12-membered [$R_4^3(12)$], and 14-membered [$R_3^3(14)$] rings (figure S6). A "head-tail" π–π stacking interaction also exists in this compound (figure S6). The distance between the rings of neighboring HTBA$^-$ anions is 3.5129 (5) Å. The powder X-ray diffraction analysis confirmed the phase homogeneity of the polycrystalline samples (figure S3).

3.3. *Crystal structure of catena-bis(2-thiobarbiturato-O,S)tetraaqua-strontium(II), 3*

The single crystal X-ray structure analysis revealed the polymer structure of **3**. The asymmetric unit consists of one Sr^{2+} cation, two HTBA$^-$ anions, and four coordinated waters (scheme 1(d) and figure 3). Each Sr^{2+} cation is eight-coordinate, from four monodentate

HTBA$^-$ ions using two O atoms and two S atoms and four water molecules, with the formation of a distorted square antiprism, as shown in figure 3. The O1, O2, O1A, and S2^i atoms make up one square of the square antiprism, and the O3, O4, O2B, and S1^{ii} atoms make up the other square (symmetry operations: (i) $1 - x$, $2 - y$, $-z$; (ii) $x - 1/2$, $3/2 - y$, $z - 1/2$). Each square antiprism is connected to three other Sr polyhedra, via the two nonequivalent μ_2-HTBA$^-$ ligands. One type of HTBA$^-$ ligand (A) forms a single bridge between two Sr^{2+} cations, while two anions of the other type (B) form a double bridge between different Sr^{2+} cations. The latter construction creates a 12-membered ring, as in **1** (figure 3). The Sr–Sr distance of 8.8641(6) Å is larger than the Ca–Ca distance in **1**, but the shapes of the rings are similar. The root mean square difference (RMS) between the rings is not large (table S2). Similar rings were also observed in other compounds found with the Mercury CSD 3.1 program. In table S2, the compounds are ordered by their RMS value. The metal–metal distances are in the range 6.49–9.56 Å and the average distance of 8 Å is close to the Sr–Sr distance in **3**. There are only nine structures with a Sr–S bond [12]. The μ_2-O,S bridging of the HTBA$^-$ ligand in **3** was not previously known for Sr(II) complexes.

The Sr–O bond distances in **3** range from 2.523(2) to 2.583(2) Å (table 2), comparable to those reported for Sr–O bonds in other eight-coordinate strontium complexes [12]. The Sr–S1 and Sr–S2 bond distances are 3.1668(7) Å and 3.3533(7) Å, respectively, similar to Sr–S bond distances found in other strontium complexes [12]. The C–O distances range from 1.261(3) to 1.274(3) Å, and the values are comparable to those in **1** and **2**. This indicates the charge delocalization in the HTBA$^-$ ligand in **3**. The C4–C5–C6 angle in the two types of HTBA$^-$ ligands [121.0(2) Å for A and 121.4(2) Å for B] corresponds to sp^2 hybridization. Also, the C4A–C5A and C5A–C6A distances [1.395(3) Å, 1.383(3) Å] and C4B–C5B and C5B–C6B distances [1.394(3) Å, 1.387(3) Å] are close to typical values for an aromatic ring. A similar geometry for the HTBA$^-$ anions has been found in ammonium [17], sodium [18], and potassium [15, 16] thiobarbiturates. Eight hydrogen bonds (table 3) generate 3-D net. All water molecules are involved in hydrogen bonding to a carbonyl O atom of a HTBA$^-$ ligand. The hydrogen bonds N–H···O, O–H···O, and N–H···S form 6-membered [$R_1^1(6)$], 8-membered [$R_2^2(8)$], and 14-membered [$R_1^2(14)$] rings, respectively (figure S7). Formation of 6-membered and 8-membered rings was detected in potassium [16], lithium, and sodium thiobarbiturates [19]. The formation of a supramolecular motif
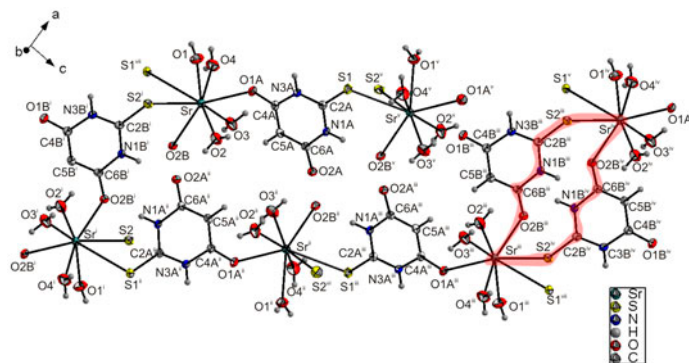

Figure 3.   Crystal structure of **3** together with the labeling scheme. Symmetry codes: (i) $1 - x$, $2 - y$, $-z$; (ii) $3/2 - x$, $\frac{1}{2} + y$, $\frac{1}{2} - z$; (iii) $2 - x$, $2 - y$, $1 - z$; (iv) $1 + x$, y, $1 + z$; (v) $\frac{1}{2} + x$, $3/2 - y$, $\frac{1}{2} + z$; (vi) $\frac{1}{2} + x$, $5/2 - y$, $\frac{1}{2} + z$; (vii) $5/2 - x$, $\frac{1}{2} + y$, $3/2 - z$. The ellipsoids are drawn at the 50% probability level. The red line shows the 12-membered ring. (see http://dx.doi.org/10.1080/19443994.2013.860450 for color version)

$R_2^2(8)$ is relatively frequent [20, 21]. A "head-tail" $\pi-\pi$ stacking interaction plays an important role in the structure of this system. The centroid–centroid and interplanar separation distances [3.80(5) and 3.49(3) Å, respectively] between the rings of two neighboring HTBA$^-$ ligands are comparable to those in potassium thiobarbiturate [18]. The SrO_6S_2 polyhedra form layers in the *ab* plane (figure S8). The layers are connected by the two nonequivalent μ_2-HTBA$^-$ anions in the 3-D network. The powder X-ray diffraction analysis indicates that the bulk material contains several phases, which could not be separated.

3.4. *IR spectroscopy*

The characteristic IR absorption bands of H$_2$TBA and **1–3** are listed in table 4. The carbonyl absorption bands v(C=O) at 1720 and 1690 cm^{-1} of H$_2$TBA [10, 22] are shifted to lower frequencies or disappear from the spectra of **1–3**. The changes in the position and intensity of the carbonyl band indicate that, at least, one of two carbonyl groups in H$_2$TBA is coordinated to the Ca^{2+} or Sr^{2+} cation. The IR spectra of **1–3** show distinct vibrational bands between 1539–1540 and 1362–1392 cm^{-1}, which are assigned to the (CN) vibrations (thioamide I and II bands), and the bands between 1173–1182 and 775–811 cm^{-1} can be attributed to the (CS) vibrations (thioamide III and IV bands). The corresponding thioamide I and II bands in crystalline H$_2$TBA appear at 1527 and 1350 cm^{-1}, while the thioamide bands III and IV are observed at 1154 and 801 cm^{-1} [11]. The shift of the thioamide III band in **3** to lower frequencies from that in H$_2$TBA supports the S-coordination of the ligand. The v(NH) band at 3109 cm^{-1} for H$_2$TBA is only slightly shifted in the spectra of **1–3**, indicating that the NH groups are not involved in bonding with the metal ions and that deprotonation of the N atoms did not occur. The broad bands at 3422–3432 cm^{-1} in the IR spectra of **1–3** are due to v(O–H) involved in hydrogen-bonding interactions. The assignment of the IR vibrational bands to the corresponding normal modes is based on the data for other thiobarbiturate complexes [11, 15, 22].

3.5. *Thermal decomposition*

The DSC and TG curves of **1** (figure S9), **2** (figure S10), and **3** (figure S11) display two distinct decomposition regions. The number of endothermic peaks in the DSC traces in the temperature range 40–275 °C corresponds to the number of dehydration processes. According to the MS data, only water ($m/z = 18$) was released at temperatures lower than 275 °C under both Ar–O$_2$ and oxygen-free atmospheres. The total weight loss Δm from 40 to 275 °C was close to the theoretical Δm value estimated from the dehydration of four and

Table 4.   Characteristic IR bands for H$_2$TBA and **1–3**.

	H$_2$TBA	**1**	**2**	**3**
v(O–H)	–	3426	3432	3422
v(N–H)	3109	3095	3078	3105
Thioamide band I	1527	1540	1540	1539
Thioamide band II	1350	1375	1362	1392
Thioamide band III	1154	1173	1182	1179
Thioamide band IV	801	792	811	775
v(C=O)	1720	1650	163	1641
	1682	1596	1600	1600

seven coordinated water molecules from **1** (experimental Δm = 18.27 %; theor. 18.09%) and **2** (exptl. 27.85%; theor. 27.88%), respectively. The most probable reason for a slight excess of H_2O content over the theoretical value for **1** is the presence of a more hydrated compound. Thermal stability of **1–3** decreases in the order **1** > **2** > **3**. Contrary to the behavior of Ca salts, the Sr thiobarbiturate was found to lose some water at room or slightly higher temperatures (~40 °C, figure S11). The total weight loss from 40 to 275 °C for **3** was as high as 17.77%. The water content (4.49 ± 0.09) determined from the TG curve is a bit larger than that expected from the structural data (4.00). This significant difference can be attributed to the presence of different hydrated complexes in the polycrystalline substance. The dehydration of **1–3** proceeds as a multi-step process. Both DSC and TG curves show peaks indicating several steps for water removal. There are two peaks observed for **1** (T_{max} at 150 and 228 °C), three for **2** (81, 139, and 220 °C), and two for **3** (112 and 177 °C). The anhydrous thiobarbiturates are stable under Ar–O_2 up to 280–290 °C. An exothermic process starts at higher temperatures, and the corresponding DSC curves (figures S9, S10, and S11) show a complex decomposition which can be conventionally divided into two steps. At the beginning of the process, an abrupt change in the sample mass occurs followed by almost continuous residue degradation. The final stage of the oxidative decomposition is a very sharp exothermic process, and the maximum of the transformation rate is located at 750–760 °C, 705–715 °C, and 580–590 °C for **1–3**, respectively. The PXRD analysis of the white powders formed after calcination at 1000 °C shows calcium or strontium sulfates and oxides as the principal constituents of the residue. The expected mass loss of the transformation of $Me(HTBA)_2 \cdot nH_2O$ to $xMeSO_4 + (1-x)MeO$ can vary in the ranges 65.83–85.93% (MeCa, n = 4), 69.9–87.6% (Me=Ca, n = 47), and 60.4–77.7% (MeSr, n = 45), depending on the x-value. The experimental values of the total mass loss are 74.71, 74.88, and 64.06% for **1–3**, respectively, which are within these intervals.

4. Conclusion

The reaction of H_2TBA with calcium and strontium carbonate leads to three new compounds, $[Ca_2(H_2O)_8(\mu_2\text{-HTBA-O,O'})_2(\text{HTBA-O})_2]$ (**1**), $[Ca(H_2O)_5(\text{HTBA-O})_2]\cdot2H_2O$ (**2**), and $[Sr(H_2O)_4(\mu_2\text{-HTBA-O,S})_2]_n$ (**3**). The binuclear Ca^{2+} cation complex (**1**) and the polymeric Sr^{2+} cation complex (**3**) were crystallized between 50 and 60 °C, and the mononuclear Ca^{2+} complex (**2**) was crystallized at 20 °C. The crystal structures of **1** and **2** show that Ca^{2+} only coordinates to O donors, with the formation of monocapped trigonal prisms. In **3**, Sr^{2+} coordinates to both S and O donors. The Sr^{2+} has a distorted square antiprism coordination geometry. The antiprisms are connected by μ_2-O,S bridging HTBA$^-$ ligands. This type of μ_2-O,S bridging ligand coordination was until now unknown in Sr(II) complexes. The HTBA$^-$ shows different coordination modes in **1–3**. In **2**, both HTBA$^-$ are O-monodentate ligands, and in **1** one HTBA$^-$ is a O-monodentate ligand, while the other is a μ_2-O,O' bridging ligand. In **3**, all HTBA$^-$ are μ_2-O,S bridging ligands. Generally, the barbiturates coordinate through deprotonated N, carbonyl O [23–25], and C, with variation in the type metal [12]. Unlike the d-elements, the alkali metals (Na, K, Rb, Cs) [26] and Ca^{2+} cations [27] connect only through the carbonyl O. However, in $[Ba_2H(Barb)_5]$ (Barb$^-$ = 5,5-diethyl barbiturate anion), Ba^{2+} is bound to the ligand through both O and N [28]. As shown in the present study, coordination of thiobarbiturate through O or O and S atoms is preferable over coordination via a N. This study clearly shows how the combination of

coordination chemistry, hydrogen bonding, and π–π stacking interactions can provide rich chemistry for alkaline-earth metals with ligands derived from deprotonated thiobarbituric acid. Infrared spectroscopy data also supported the crystal structure data. Thermal stability of **1–3** decreases in the order **1 > 2 > 3**. The dehydration was a multi-step process followed by exothermic oxidative degradation of the 2-thiobarbiturate moiety between 290 and 800 °C.

Supplementary material

Tables of metal–metal distances in structures related to **1–3** [29–45]; IR spectra of **1–3**; PXRD patterns of **1–3**; figures of the extended and hydrogen-bonding structures and π–π stacking interactions of **1–3**; figures of the TG-DSC data for **1–3**. Crystallographic data (excluding structure factors) for the structural analysis have been deposited with the Cambridge Crystallographic Data Center, Nos. CCDC-910776 (**1**), CCDC-941788 (**2**) and CCDC-916454 (**3**). The information copies may be obtained free of charge from The Director, CCDC, 12 Union Road, Cambridge CB2 1EZ, UK (Fax: +44(1223)336-033, E-mail: deposit@ccdc.cam.ac.uk, or www: http://www.ccdc.cam.ac.uk).

Supplemental data

Supplemental data for this article can be accessed http://dx.doi.org/10.1080/19443994.2013.860450.

References

[1] B.R. Srinivasan, S.Y. Shetgaonkar. *J. Coord. Chem.*, **63**, 3403 (2010).
[2] K.M. Fromm. *Coord. Chem. Rev.*, **252**, 856 (2008).
[3] W.J. Hunks, M.C. Jennings, R.J. Puddephatt. *Inorg. Chem.*, **41**, 4590 (2002).
[4] D.J. Tranchemontagne, J.L. Mendoza-Cortes, M. O'Keeffe, O.M. Yaghi. *Chem. Soc. Rev.*, **38**, 1257 (2009).
[5] S. Natarajan, J.K. Sundar, S. Athimoolam, B.R. Srinivasan. *J. Coord. Chem.*, **64**, 2274 (2011).
[6] K. Biradha, A. Ramanan, J.J. Vittal. *Cryst. Growth Des.*, **9**, 2969 (2009).
[7] S. Bondock, T.A. El-Gaber, A.A. Fadda. *Phosphorus Sulfur Silicon Relat. Elem.*, **182**, 1915 (2007).
[8] J. Karthikeyan, P. Parameshwara, A.N. Shetty, P. Shetty. *Indian J. Chem. Technol.*, **15**, 186 (2008).
[9] E.R. Milaeva, V.-Y. Tyurin, D.B. Shpakovsky, O.A. Gerasimova, Z. Jingwei, Y.A. Gracheva. *Heteroat. Chem.*, **17**, 475 (2006).
[10] M.R. Chierotti, L. Ferrero, N. Garino, R. Gobetto, L. Pellegrino, D. Braga, F. Grepioni, L. MainiL. *Chem. Eur. J.*, **16**, 4347 (2010).
[11] E. Mendez, M.F. Cerda, J.S. Gancheff, J. Torres, C. Kremer, J. Castiglioni, M. Kieninger, O.N. Ventura. *J. Phys. Chem. C*, **111**, 3369 (2007).
[12] F.H. Allen. *Acta Cryst. B*, **58**, 380 (2002).
[13] M.S. Masoud, E.A. Khalil, A.M. Hindawy, A.E. Ali, E.F. Mohamed. *Spectrochim. Acta, Part A*, **60**, 2807 (2004).
[14] G.M. Sheldrick, *SHELXS and SHELXL97, Program for Crystal Structure Refinement*, University of Göttingen, Germany (1997).
[15] M. Kubicki, A. Owczarzak, V.I. Balas, S.K. Hadjikakou. *J. Coord. Chem.*, **65**, 1107 (2012).
[16] N.N. Golovnev, M.S. Molokeev. *Russ. J. Struct. Chem.*, **54**, 521 (2013).
[17] R. Betz, T. Gerber. *Acta Crystallogr. E*, **66**, 1326 (2011).
[18] B. Li, W. Li, L. Ye, G.-F. Hou, L.-X. Wu. *Acta Crystallogr. E*, **66**, 1546 (2010).
[19] N.N. Golovnev, A.D. Vasiliev, S.D. Kirik. *J. Mol. Struct.*, **1021**, 112 (2012).
[20] A.D. Vasiliev, N.N. Golovnev. *Russ. J. Struct. Chem.*, **52**, 818 (2011).
[21] N.N. Golovnev, M.S. Molokeev. *Acta Crystallogr C*, **69**, 704 (2013).
[22] M.S. Refat, S.A. El-Korashyb, A.S. Ahmed. *Spectrochim. Acta, Part A*, **71**, 1084 (2008).
[23] F. Yilmaz, V.T. Yilmaz, E. Biger, O. Buyukgungor. *J. Coord. Chem.*, **60**, 777 (2007).
[24] M.S. Aksoy, V.T. Yilmaz, O. Buyukgungor. *J. Coord. Chem.*, **62**, 3250 (2009).
[25] V.T. Yilmaz, F. Yilmaz, E. Guney, O. Buyukgungor. *J. Coord. Chem.*, **64**, 159 (2011).

[26] D. Braga, F. Grepioni, L. Maini, S. Prosperi, R. Gobetto, M.R. Chierotti. *Chem. Commun.*, **46**, 7715 (2010).

[27] D. Braga, F. Grepioni, L. Maini, G.I. Lampronti, D. Capucci, C. Cuocci. *CrystEngComm.*, **14**, 3521 (2012).

[28] M.M. Ibrahim, S. Al-Juaid, M.A. Mohamed, M.H. Yassin. *J. Coord. Chem.*, **65**, 2957 (2012).

[29] G.S. Nichol, W. Clegg, M.J. Gutmann, D.M. Tooke. *Acta Crystallogr., Sect. B*, **62**, 798 (2006).

[30] B.-J. Deelman, F. Wierda, A. Meetsma, J.H. Teuben. *Appl. Organomet. Chem.*, **9**, 483 (1995).

[31] P.S. Pereira Silva, M. Ramos Silva, J.A. Paixão, A. Matos Beja. *J. Chem. Crystallogr.*, **39**, 669 (2009).

[32] E. Freisinger, A. Schimanski, B. Lippert. *JBIC J. Biol. Inorg. Chem.*, **6**, 378 (2001).

[33] B. Briggman, A.A. Oskarsson. *Acta Crystallogr., Sect. B*, **33**, 1900 (1977).

[34] G.S. Nichol, W. Clegg. *Acta Crystallogr., Sect. C*, **61**, m459 (2005).

[35] V.T. Yilmaz, F. Yilmaz, H. Karakaya, O. Büyükgüngör, W.T.A. Harrison. *Polyhedron*, **25**, 2829 (2006).

[36] K. Matlawska, U. Kalinowska, A. Erxleben, R. Osiecka, J. Ochocki. *Eur. J. Inorg. Chem.*, **2005**, 3109 (2005).

[37] M.L. Godino Salido, P. Arranz Mascarós, R. López Garzón, M.D. Gutiérrez Valero, J.N. Low, J.F. Gallagher, C. Glidewell. *Acta Crystallogr., Sect. B*, **60**, 46 (2004).

[38] R. Fischer, M. Gärtner, H. Görls, L. Yu, M. Reiher, M. Westerhausen. *Angew. Chem. Int. Ed.*, **46**, 1618 (2007).

[39] Y. Suenaga, T. Kuroda-Sowa, M. Maekawa, M. Munakata. *J. Chem. Soc., Dalton Trans.*, 2737 (1999).

[40] J.D. Owen. *J. Chem. Soc., Perkin Trans.*, **2**, 407 (1983).

[41] B.-H. Zhu, Y. Shibata, S. Muratsugu, Y. Yamanoi, H. Nishihara. *Angew. Chem. Int. Ed.*, **48**, 3858 (2009).

[42] D.A. Dickie, M.V. Parkes, R.A. Kemp. *Angew. Chem. Int. Ed.*, **47**, 9955 (2008).

[43] H. Preut, K. Grätz, F. Huber. *Acta Crystallogr., Sect. C*, **40**, 941 (1984).

[44] M. Munakata, L. Ping Wu, T. Kuroda-Sowa, M. Maekawa, Y. Suenaga, K. Sugimoto, I. Ino. *J. Chem. Soc., Dalton Trans.*, 373 (1999).

[45] N.J. Ray, B.J. Hathaway. *Acta Crystallogr., Sect. B*, **38**, 770 (1982).